PHYSICAL REVIEW E **95**, 060202(R) (2017)

Intermittent many-body dynamics at equilibrium

C. Danieli,[1,2] D. K. Campbell,[3] and S. Flach[2,1]

[1]*New Zealand Institute for Advanced Study, Centre for Theoretical Chemistry & Physics, Massey University, Auckland 0745, New Zealand*

[2]*Center for Theoretical Physics of Complex Systems, Institute for Basic Science, Daejeon 34051, Korea*

[3]*Department of Physics, Boston University, Boston, Massachusetts 02215, USA*

(Received 1 November 2016; revised manuscript received 11 February 2017; published 2 June 2017)

The equilibrium value of an observable defines a manifold in the phase space of an ergodic and equipartitioned many-body system. A typical trajectory pierces that manifold infinitely often as time goes to infinity. We use these piercings to measure both the relaxation time of the lowest frequency eigenmode of the Fermi-Pasta-Ulam chain, as well as the fluctuations of the subsequent dynamics in equilibrium. The dynamics in equilibrium is characterized by a power-law distribution of excursion times far off equilibrium, with diverging variance. Long excursions arise from sticky dynamics close to q-breathers localized in normal mode space. Measuring the exponent allows one to predict the transition into nonergodic dynamics. We generalize our method to Klein-Gordon lattices where the sticky dynamics is due to discrete breathers localized in real space.

DOI: 10.1103/PhysRevE.95.060202

Equipartition and thermalization have been central research topics in many-body interacting systems since the time of Maxwell, Boltzmann, and Gibbs. The first computer experiment, aimed to observe equipartition starting from a microscopic reversible dynamical system, was carried out in the 1950's by Fermi, Pasta, Ulam, and Tsingou [1]. Now famous as the Fermi-Pasta-Ulam (FPU) paradox (for reviews, see Refs. [2–5]), this experiment failed to find equipartition but instead revealed intriguing nonlinear dynamics—including the celebrated *FPU recurrences* [1]—which has challenged and puzzled researchers for more than 60 years (for a recent survey of the state of the art, see Ref. [4]). In brief, attempts to understand the full dynamics, including the recurrences, led to the observation (and naming) of *solitons* [6,7] and important developments in Hamiltonian chaos [8]. It is now known that these unexpected recurrences are linked to the choice of initial conditions used by FPU, which are set close to exact coherent time-periodic (or even quasiperiodic) trajectories, e.g., *q-breathers*, which show exponential localization of energy in *normal mode space* [9,10]. Even if these trajectories have support of measure zero in the phase space, they might have a finite measure impact simply by being linearly stable [9]. Several other studies admit coherent time-periodic states localized in real space, which are known as *discrete breathers* or *intrinsic localized modes* [11] and exist, e.g., in Klein-Gordon (KG) lattices [12]. These states can also be linearly stable and thus may have finite measure impact. Importantly, both discrete breathers and q-breathers have been experimentally observed in a large variety of physical settings [11,13]. Thus the central question becomes: How does the presence of such coherent states of measure zero affect the dynamical properties of a *thermalized* many-body system? How do they affect the possible transition from ergodic to a nonergodic dynamics? Interestingly, there are only a few recorded numerical attempts to address this complex issue [14–21]. In our view, this is the result of the lack of a clear strategy which can go beyond the analysis of correlation functions (which obscure the understanding of a detailed correspondence between the equilibrium dynamics and coherent structures due to event averaging).

Given a many-body system which possesses linearly stable coherent states, we choose an observable f (i.e., some function of the phase space variables) whose value is sensitive to the excitation of such states. We assume that the many-body system is thermalizing, or ergodic, i.e., that the phase space trajectory is evolving under the constraint of fixed total energy (and perhaps other conserved quantities) such that the time average $\langle f\rangle_t \equiv \langle f\rangle$ is independent of the actual chosen trajectory, up to a set of measure zero (such as periodic orbits, which can persist even in the strongest chaotic flows). The actual value of $f(t)$ will depend upon time t along a typical trajectory. As time goes to infinity, the trajectory is then forced to pierce infinitely often a submanifold $\mathcal{F}_f$ of codimension 1 which hosts all phase space points with $f \equiv \langle f\rangle$. The submanifold can be considered as a generalized ergodic Poincaré section, which is fixed by the choice of f, the integrals of motion, and the assumption of ergodicity. The time intervals between consecutive piercings will carry the information on whether (and when) the trajectory was visiting a sticky region in phase space. Hence we will study the statistics of these time intervals. In contrast to a correlation function, these are the statistics of trackable events and will always permit us to return to the event of interest, in order to inspect it microscopically. With this insight we also arrive at a quantitative dynamical characterization of the degree of equipartition of a given microscopical state, i.e., a point on the considered trajectory. Rather than using an entropylike measure (e.g., the distance from the set $\mathcal{F}_f$), it is the time the trajectory needs to reach and pierce $\mathcal{F}_f$ which will decide whether the given configuration is close to or far from equilibrium.

We apply the above ideas to both FPU and KG systems with the Hamiltonian function of the canonically conjugated pairs of real space momenta and coordinates $\{p_n,q_n\}$,

$$H = \sum_{n=0}^{N}\left[\frac{p_n^2}{2} + V(q_n) + W(q_{n+1}-q_n)\right], \qquad (1)$$

$$\text{FPU:}\quad V(q)=0,\quad W(q)=\frac{1}{2}q^2+\frac{\alpha}{3}q^3, \qquad (2)$$

$$\text{KG:}\quad V(q)=\frac{1}{2}q^2+\frac{1}{4}q^4,\quad W(q)=\frac{k}{2}q^2. \qquad (3)$$

Both models turn into integrable sets of noninteracting normal modes in the limit of vanishing energies. In addition, the

KG system turns into an integrable set of noninteracting anharmonic oscillators in the limit of diverging energies, due to its on-site anharmonicity (as opposed to the FPU case). We use fixed boundary conditions $p_0 = p_{N+1} = q_0 = q_{N+1} = 0$ for the FPU chain in line with Ref. [1]. For the KG chain we use instead periodic boundary conditions $p_1 = p_{N+1}$, $q_1 = q_{N+1}$ in order to keep all sites equivalent and to avoid edge effects.

To address the normal mode dynamics, we use the FPU system and the canonical transformation

$$\begin{pmatrix} P_k \\ Q_k \end{pmatrix} = \sqrt{\frac{2}{N+1}} \sum_{n=1}^{N} \begin{pmatrix} p_n \\ q_n \end{pmatrix} \sin\left(\frac{\pi n k}{N+1}\right), \tag{4}$$

with $k = 1, \ldots, N$, which diagonalizes the harmonic part of H [$\alpha = 0$ in (2)] with the normal mode momenta and coordinates $\{P_k, Q_k\}$. The mode energies and frequencies are

$$E_k = \frac{P_k^2 + \omega_k^2 Q_k^2}{2}, \quad \omega_k = 2\sin\left(\frac{\pi k}{2(N+1)}\right). \tag{5}$$

For $\alpha \neq 0$ the mode energies become time dependent and are monitored using the normalized distribution $\nu_k(t) = E_k(t)/\sum_{k=1}^{N} E_k(t)$, with $\sum_k \nu_k = 1$. A common tool to monitor the degree of inhomogeneity of the distribution is the spectral entropy [22,23]

$$S(t) = -\sum_{k=1}^{N} \nu_k(t) \ln[\nu_k(t)], \tag{6}$$

with $0 \leqslant S \leqslant S_{\max} = \ln N$. Its rescaled analog is

$$\eta(t) = \frac{S(t) - S_{\max}}{S(0) - S_{\max}}, \quad 0 \leqslant \eta \leqslant 1\ . \tag{7}$$

To address the real space dynamics of the KG system, we use the energy densities

$$\epsilon_n = \frac{p_n^2}{2} + V(q_n) + \frac{k}{4} \sum_{s=\pm 1} W(q_{n+s} - q_n). \tag{8}$$

An equally common measure of energy distribution inhomogeneity is the participation number P, which yields the number of strongly excited renormalized energies $\mu_n(t) = \epsilon_n(t)/\sum_{n=1}^{N} \epsilon_n(t)$:

$$P^{-1}(t) = \sum_{n=1}^{N} \mu_n^2(t), \quad 1 \leqslant P \leqslant N. \tag{9}$$

Both observables η and P^{-1} will fluctuate along the temporal evolution of a trajectory. Let us assume that their averages $\langle \eta \rangle, \langle P^{-1} \rangle$ exist and can be computed using the Gibbs distribution (which follows from well-known general considerations of counting microstates or maximizing the entropy)

$$W_B = \frac{1}{Z} e^{-\beta H}, \quad Z = \int_{\Gamma} e^{-\beta H} d\Gamma. \tag{10}$$

Here, Γ denotes the whole available phase space, and β is the inverse temperature. At low enough energies the anharmonic energy contribution for the FPU system will be a small correction and can be neglected when computing averages; its relevance is reduced to the highly important nonlinear mode interaction which is the crucial source of deterministic chaos and equipartition. The final integration using the Gibbs distribution (10) can be performed analytically [24],

$$\langle \eta \rangle = \frac{1 - \gamma}{\ln N - S(0)}, \tag{11}$$

where $\gamma \approx 0.5772$ is the Euler constant. For the KG system, we obtain the average $\langle P^{-1} \rangle$ directly by numerically averaging until the total integration time $T = 10^8$. These averages define the equilibrium manifolds $\mathcal{F}_\eta, \mathcal{F}_P$ which we will use for the subsequent analysis.

The original FPU computation [1] was performed for $N = 32$ particles with only the lowest frequency mode excited, $Q_1 \neq 0$ only. Then $S(0) = 0$ and $\langle \eta \rangle \approx 0.1218$. We will benchmark our data with the results from Ref. [22], who used an *ad hoc* value $\eta = 0.1$. The trajectory starts with $\eta(0) = 1 \gg \langle \eta \rangle$, close to a regular periodic orbit localized in momentum space (a q-breather) [9]. A central target of many FPU paradox studies was to quantify the time this initial state needs to reach equipartition, if it ever does (e.g., Refs. [1,22,23,25,26]). Since equipartition means equal mode energies on average, we define the FPU equipartition time $T_{\rm FPU}$ as the time the trajectory needs to reach the corresponding manifold $\mathcal{F}_\eta$. We continue our computations beyond this equipartition time. The trajectory has to cross the manifold $\mathcal{F}_\eta$ infinitely often, and we record the piercing times t_i with $i \geqslant 1$ (note that $T_{\rm FPU} \equiv t_1$). The *return times*

$$t_r(i) = t_{i+1} - t_i, \quad i \geqslant 1, \tag{12}$$

measure the time intervals the trajectory spends off the equilibrium manifold before piercing it again, with even and odd integers i discriminating between corresponding excursions into the two different phase space subspaces (e.g., $\eta > \langle \eta \rangle$ and $\eta < \langle \eta \rangle$).

The computations were carried out using a symplectic $SABA_2C$ integrator with a corrector with a time step $\tau = 0.1$; these choices keep the relative energy error of the order 10^{-5} [27,28]. The system size is $N = 32$, and $\alpha = 0.25$ in Eq. (2), and initial condition $P_k(0) = 0$, $Q_k(0) = A\delta_{k,1}$, which translates into a corresponding total energy E, and energy density $\epsilon = E/N$. We follow the time dependence of observables and also perform a window averaging over a time window which is 100 times shorter than the actual running time.

In Fig. 1(a) we show the time evolution of the entropy η for different energy densities ϵ. The curves start at the unity at $t = 0$ [see Eq. (7)] and then settle to fluctuating intermediate values for a transient interval of time that increases as the energy density ϵ decreases. Finally, at $t = T_{\rm FPU}$ the observable transits into fluctuations around equilibrium at values that approximate the Gibbs average $\langle \eta \rangle$ very well. The intermediate plateau corresponds to a *metastable* state, where all the mode energies E_k are nonzero but assume an exponentially decaying profile [4,26,29,30]. The second plateau corresponds to the regime of equipartition, confirming the validity of the Gibbs distribution.

In Fig. 1(b) we plot the FPU equipartition time $T_{\rm FPU}$ as a function of the density ϵ, along with the data from Ref. [22], which show very good agreement. We also satisfactorily compared our data to the extrapolated equipartition times from Ponno *et al.* [26] (see details in Ref. [31]). As noted previously, the equipartition time increases with decreasing energy density. Casetti *et al.* predicted the equipartition time

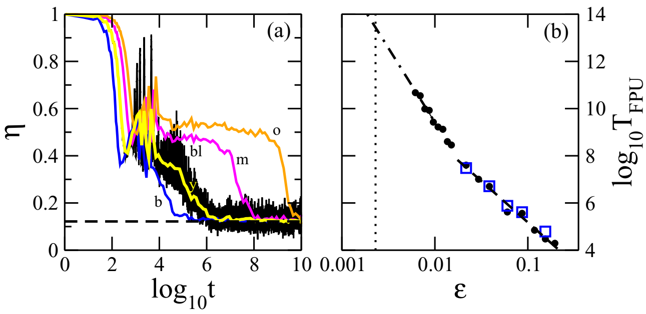

FIG. 1. (a) Instantaneous (black [bl]) and window-averaged (yellow [y]) time evolution of the entropy η for $\epsilon = 0.0566$. From top to bottom: Window-averaged time evolution for $\epsilon = 0.0091$ (orange [o]), $\epsilon = 0.0204$ (magenta [m]), $\epsilon = 0.0566$ (yellow [y]), and $\epsilon = 0.145$ (blue [b]). Black dashed line: $\langle \eta \rangle = 0.1218$. (b) $T_{\rm FPU}$ (black circles) vs ϵ. The blue squares are the data from Ref. [22]. The black dashed and dashed-dotted lines guide the eye and indicate a crossover at $\epsilon \approx 0.01$. Vertical dotted line: $\epsilon = 0.0023$.

at the original FPU energy density choice of $\epsilon = 0.002\,26$ to be of the order of $T_{\rm FPU} \approx 10^{12}$ which currently requires about 30 days of CPU time with our system [32]. However, the equipartition time shows a crossover at $\epsilon \approx 0.01$, which was not reached by previous computations. A straightforward extrapolation from this crossover [see the dashed-dotted line in Fig. 1(a)] increases this time to $T_{\rm FPU} \approx 10^{14}$ or about 10 years of CPU time on our system. Remarkably, the answer to whether the original FPU trajectory is or is not thermalizing remains a very hard computational problem more than six decades after the first observation of the FPU paradox.

Let us now turn to the analysis of the equilibrium dynamics beyond the equipartition time. We compute the sets of return times (12) separately for the two different subspaces $\eta > \langle \eta \rangle$ and $\eta < \langle \eta \rangle$. The probability distribution functions (PDFs) of these sets $\mathcal{P}_\pm(t_r)$ are shown for $\epsilon = 0.0566$ in Fig. 2(a).

In the subspace $\eta > \langle \eta \rangle$, the dynamics exhibits algebraic tails in the PDF $\mathcal{P}_+(t_r) \sim t_r^{-\delta}$ with an exponent $2 < \delta < 3$, which indicates a finite average (first moment) $\langle t_r \rangle$ but a diverging variance (second moment) $\langle t_r^2 \rangle$ (see Ref. [31] on the numerical details of estimating δ). The exponent δ decreases with decreasing energy density ϵ, signaling the reaching of the integrable harmonic oscillator chain limit. Note that for $\delta \leqslant 2$ the average $\langle t_r \rangle$ would diverge, and the ergodicity assumption would be violated, again indicating the transition into a nonergodic, perhaps integrable, case. Therefore, our method is sensitively predicting the transition from ergodic to nonergodic dynamics. In contrast, the subspace $\eta < \langle \eta \rangle$ dynamics yields tails in $\mathcal{P}_-(t_r)$ with finite moments; the tails are faster than algebraic but slower than exponential, presumably exponentials dressed with a power law. This is due to that subspace hosting microstates for which the normal modes are even more equipartitioned than on a Gibbs average. Such microstates have small probability, and are insensitive for detecting nonequilibrium fluctuations.

We extend the analysis of the dynamics at equipartition and the distribution of the return times to the KG chain, a model known to possess a discrete breather solution in the real space [12], and should show a related transition to nonergodicity and integrability with increasing energy density.

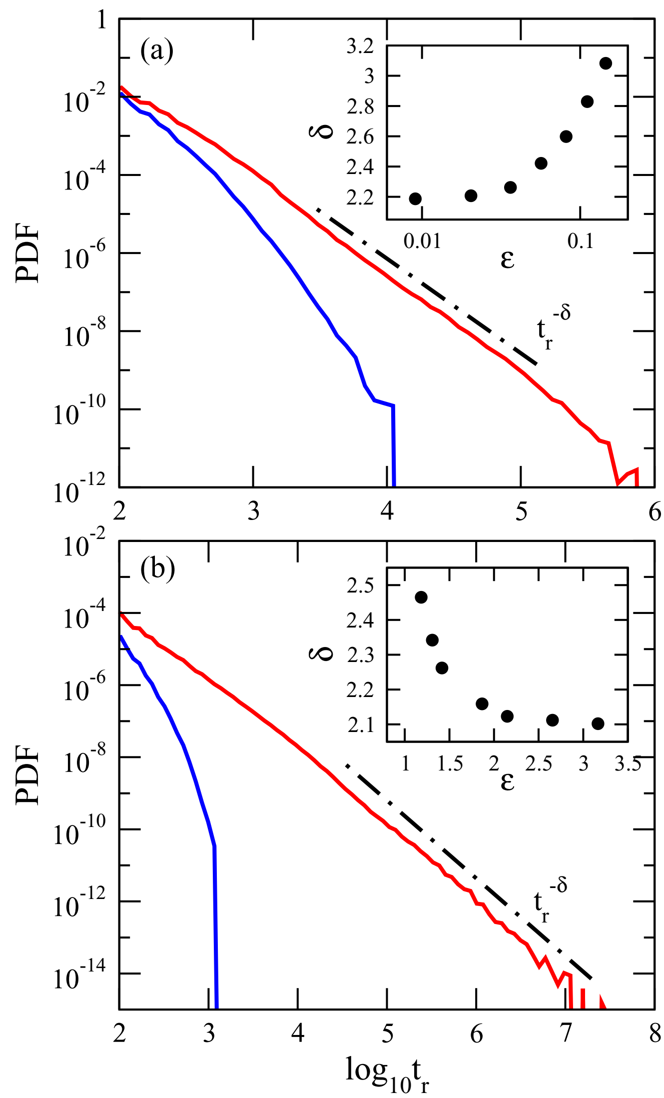

FIG. 2. PDFs $\mathcal{P}_\pm(t_r)$ for $\epsilon = 0.0566$ [(a) FPU] and $\epsilon = 1.867$ [(b) KG]. For both FPU and KG, the red (upper) curve corresponds to $\mathcal{P}_+(t_r)$ and the blue (bottom) one to $\mathcal{P}_-(t_r)$. The dashed-dotted lines guide the eye and indicate the algebraic tails. Inset: The exponent δ of the algebraic tails vs the energy density ϵ.

At variance to the FPU case, we will search for a gradual loss of ergodicity upon *increasing* the energy density, which should favor the excitations of discrete breathers. We choose $N = 32$, $k = 0.1$, periodic boundary conditions, and random initial conditions with a predefined energy density. We compute the time evolution of the participation ratio P until total integration time $T = 10^{10}$, and we record the return times t_r between two consecutive piercings of the equilibrium manifold $\mathcal{F}_P$ again separating the phase space in $P^{-1} > \langle P^{-1} \rangle$ and $P^{-1} < \langle P^{-1} \rangle$. The PDFs $\mathcal{P}_\pm(t_r)$ obtained for energy density $\epsilon = 1.867$ are shown in Fig. 2(b), where, for $P^{-1} > \langle P^{-1} \rangle$, the algebraic tail of $\mathcal{P}_+(t_r) \sim t_r^{-\delta}$ is visible while $\mathcal{P}_-(t_r)$ shows exponential cutoff. In the inset we plot the exponent δ, which drops below values of $\delta = 3$ and continues to decrease towards the critical case $\delta = 2$ with increasing energy density ϵ. Similar to the FPU case, the KG system dynamics shows a transition from ergodic into nonergodic dynamics.

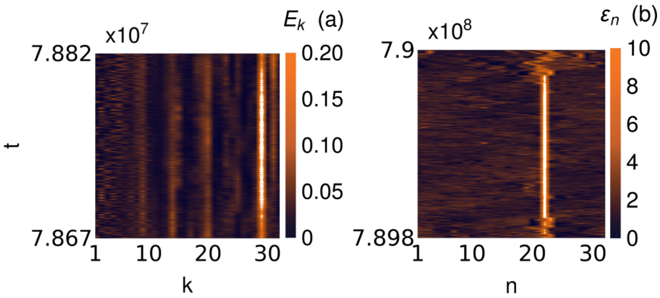

FIG. 3. (a) Mode energies E_k of the FPU as function of time during one of the longest trapping events for $\epsilon = 0.0566$. (b) Energy densities ϵ_n of the KG as a function of time during one of the longest trapping events for $\epsilon = 1.748$.

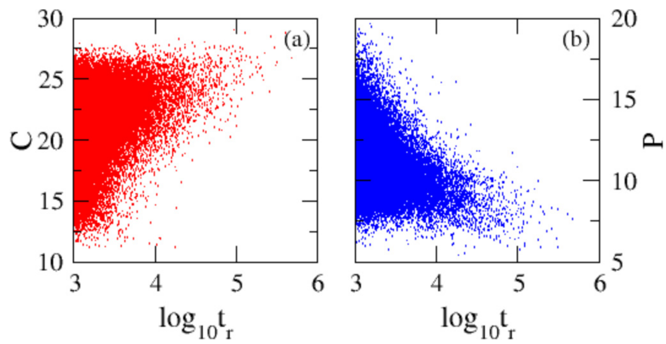

FIG. 4. (a) $C(t_r)$ and (b) $P(t_r)$ for $\epsilon = 0.0566$ (see text for details). The broad scattering of data is due to many independent events yielding similar return times t_r.

The algebraic tails of the PDF of the return times with $3 > \delta > 2$ imply that the trajectory is with high probability getting trapped in some parts of phase space for long times, whose average is finite, but whose variance diverges. We conjecture that these trapping events are due to visiting regions of the phase space which are substantially close to some regular orbits. In order to substantiate this conjecture, we show in Fig. 3 the time evolution of the mode energies E_k [Fig. 3(a), FPU] and the energy densities ϵ_n [Fig. 3(b), KG] during one of their longest excursions far from equilibrium. At the beginning of the event we observe the focusing of energy in one of the modes (FPU) or sites (KG), respectively. These breatherlike excitations then survive over the entire duration of the excursion, only to dissolve their energy back into the other degrees of freedom at the end of the event.

To further substantiate our observation, we show the correlation between the first moment of the event-averaged mode energy distribution $C = \sum_{k=1}^{N} k\nu_k$ for the FPU case versus the trapping event time t_r.

In Fig. 4(a), we observe that large return times t_r imply large values of $C \approx N$, signaling a tendency towards high frequency excitations. Most importantly, the corresponding computation of the participation number P of the event-averaged mode energy distributions in Fig. 4(b) shows that large return times correlate with smaller values of P, a typical case of strongly inhomogeneous distributions. Therefore, the equilibrium FPU dynamics produces sticky excursions with long duration to strongly excited high frequency modes.

The properties of fluctuations in equilibrium should not depend on the choice of the trajectory, in accord with the assumption of equipartition and ergodicity. We tested that in the FPU chain by launching various other trajectories, e.g., exciting one high frequency mode, or several modes with different frequencies (not shown here). We observed that the statistics of return times is universal and not depending on the choice of the initial state.

Algebraic tails in correlation functions or distributions of trapping times have been previously studied for low-dimensional dynamical systems with a mixed phase space [33,34], and related to the hierarchic fractal structure of the phase space at regular island boundaries, similar to the phenomenological approach to understand glassy dynamics. However, higher phase space dimensions destroy the simple mixed phase space picture, preventing the use of this simple argument for the observation of algebraic tails [35]. In the present work we derive a well-defined sectioning at equilibrium, and a clear interpretation of the presence of algebraic tails in terms of temporal excitation of coherent states, such as time-periodic q-breathers. The large phase space dimension does not easily allow one to connect to the physics of glasses, since the potential functions are smooth, and invariant regular trajectories. Instead, we are in need of a different understanding how regular states of measure zero (e.g., time-periodic solutions) can act as dynamical barriers and bottlenecks in high-dimensional phase spaces.

We arrived at a general method to analyze the relaxation from nonequilibrium states and the equilibrium fluctuations of interacting many-body systems. The essence is to identify the relevant coherent excitations which will be the cause of stickiness, and to choose a proper observable f which can detect these events. The corresponding equilibrium value $\langle f \rangle$ defines the codimension 1 equilibrium manifolds, and the subsequent statistical analysis of the distributions of equilibrium fluctuations. When algebraic tails are observed in contrast to exponential cutoffs, the divergence of suitably high moments of the distribution indicates sticky dynamics. When the exponent $\delta < 3$, the nonequilibrium excursions into sticky events start to dominate the dynamics. Finally, when $\delta \leqslant 2$, the first moment diverges, indicating the loss of ergodicity altogether. We expect therefore that our method can be used for a broad set of other cases where nonergodic fluctuations affect the dynamics of many-body systems, such as ultracold atomic gases in optical potentials approximated by the discrete Gross-Pitaevsky equation, or networks of weakly interacting superconducting grains, among others.

We thank P. Jeszinszki and I. Vakulchyk for helpful discussions on computational aspects. The authors acknowledge financial support from IBS (Project Code No. IBS-R024-D1).

[1] E. Fermi, J. Pasta, and S. Ulam, Los Alamos Report LA-1940, 1955 (unpublished); in *Collected Papers of Enrico Fermi*, edited by E. Segré (University of Chicago Press, Chicago, 1965), Vol. 2, p. 978.

[2] J. Ford, The Fermi-Pasta-Ulam problem: Paradox turns discovery, Phys. Rep. **213**, 271 (1992).

[3] T. P. Weissert, *The Genesis of Simulation in Dynamics: Pursuing the Fermi-Pasta-Ulam Problem* (Springer, New York, 1997).

[4] *The Fermi-Pasta-Ulam Problem: A Status Report*, edited by G. Gallavotti (Springer, New York, 2008).

[5] M. A. Porter, N. J. Zabusky, B. Hu, and D. K. Campbell, Fermi, Pasta, Ulam and the birth of experimental mathematics, Am. Sci. **97**, 214 (2009).

[6] N. J. Zabusky and M. D. Kruskal, Interaction of "Solitons" in a Collisionless Plasma and the Recurrence of Initial States, Phys. Rev. Lett. **15**, 240 (1965).

[7] N. J. Zabusky and G. S. Deem, Dynamics of nonlinear lattices I. Localized optical excitations, acoustic radiation, and strong nonlinear behavior, J. Comput. Phys. **2**, 126 (1967).

[8] F. V. Izrailev and B. V. Chirikov, Statistical properties of a nonlinear string, Sov. Phys. Dokl. **11**, 57 (1966).

[9] S. Flach, M. V. Ivanchenko, and O. I. Kanakov, q-Breathers and the Fermi-Pasta-Ulam Problem, Phys. Rev. Lett. **95**, 064102 (2005); q-breathers in Fermi-Pasta-Ulam chains: Existence, localization, and stability, Phys. Rev. E **73**, 036618 (2006).

[10] H. Christodoulidi, C. Efthymiopoulos, and T. Bountis, Energy localization on q-tori, long term stability, and the interpretation of the FPU paradox, Phys. Rev. E **81**, 016210 (2010).

[11] S. Flach and C. R. Willis, Discrete breathers, Phys. Rep. **295**, 181 (1998); S. Flach and A. Gorbach, Discrete breathers: Advances in theory and applications, *ibid.* **467**, 1 (2008); D. K. Campbell, S. Flach, and Y. S. Kivshar, Localizing energy through nonlinearity and discreteness, Phys. Today **57**, 43 (2004).

[12] M. V. Ivanchenko, O. I. Kanakov, V. D. Shalfeev, and S. Flach, Discrete breathers in transient processes and thermal equilibrium, Physica D **198**, 120 (2004).

[13] M. Wu and C. E. Patton, Experimental Observation of Fermi-Pasta-Ulam Recurrence in a Nonlinear Feedback Ring System, Phys. Rev. Lett. **98**, 047202 (2007); A. Mussot, A. Kudlinski, M. Droques, P. Szriftgiser, and N. Akhmediev, Fermi-Pasta-Ulam Recurrence in Nonlinear Fiber Optics: The Role of Reversible and Irreversible Losses, Phys. Rev. X **4**, 011054 (2014).

[14] D. Escande, H. Kantz, R. Livi, and S. Ruffo, Self-consistent check of the validity of Gibbs calculus using dynamical variables, J. Stat. Phys. **76**, 605 (1994).

[15] G. P. Tsironis and S. Aubry, Slow Relaxation Phenomena Induced by Breathers in Nonlinear Lattices, Phys. Rev. Lett. **77**, 5225 (1996).

[16] K. O. Rasmussen, T. Cretegny, P. G. Kevrekidis, and N. Gronbech-Jensen, Statistical Mechanics of a Discrete Nonlinear System, Phys. Rev. Lett. **84**, 3740 (2000).

[17] M. Eleftheriou, S. Flach, and G. P. Tsironis, Breathers in 1D nonlinear thermalized lattice with an energy gap, Physica D **186**, 20 (2003); M. Eleftheriou and S. Flach, Discrete breathers in thermal equilibrium: Distributions and energy gaps, *ibid.* **202**, 142 (2005); Interaction of discrete breathers with thermal fluctuations, Low Temp. Phys. **34**, 554 (2008).

[18] H. J. Matsuyama and T. Konishi, Multistage slow relaxation in a Hamiltonian system: The Fermi-Pasta-Ulam model, Phys. Rev. E **92**, 022917 (2015).

[19] Z. Zhang, C. Tang, and P. Tong, Dynamical thermalization of Frenkel-Kontorova model in the thermodynamic limit, Phys. Rev. E **93**, 022216 (2016).

[20] C. Mulhern, S. Bialonski, and H. Kantz, Extreme events due to localization of energy, Phys. Rev. E **91**, 012918 (2015).

[21] B. Gershgorin, Y. V. Lvov, and D. Cai, Renormalized Waves and Discrete Breathers in β-Fermi-Pasta-Ulam Chains, Phys. Rev. Lett. **95**, 264302 (2005).

[22] L. Casetti, M. Cerruti-Sola, M. Pettini, and E. G. D. Cohen, The Fermi-Pasta-Ulam problem revisited: Stochasticity thresholds in nonlinear Hamiltonian systems, Phys. Rev. E **55**, 6566 (1997).

[23] M. Onorato, L. Vozella, D. Proment, and Y. V. Lvov, Route to thermalization in the α-Fermi-Pasta-Ulam system, Proc. Natl. Acad. Sci. USA **112**, 4208 (2015).

[24] C. G. Goedde, A. J. Lichtenberg, and M. A. Lieberman, Chaos and the approach to equilibrium in a discrete sine-Gordon equation, Physica D **59**, 200 (1992).

[25] J. De Luca, A. J. Lichtenberg, and S. Ruffo, Finite times to equipartition in the thermodynamic limit, Phys. Rev. E **60**, 3781 (1999).

[26] A. Ponno, H. Christodoulidi, Ch. Skokos, and S. Flach, The two-stage dynamics in the Fermi-Pasta-Ulam problem: From regular to diffusive behavior, Chaos **21**, 043127 (2011).

[27] J. Laskar and P. Robutel, High order symplectic integrators for perturbed Hamiltonian systems, Celest. Mech. Dyn. Astron. **80**, 39 (2001).

[28] Ch. Skokos, D. O. Krimer, S. Komineas, and S. Flach, Delocalization of wave packets in disordered nonlinear chains, Phys. Rev. E **79**, 056211 (2009).

[29] G. Benettin and A. Ponno, Time-scales to equipartition in the Fermi-Pasta-Ulam problem: finite-size effects and thermodynamic limit, J. Stat. Phys. **144**, 793 (2011).

[30] F. Fucito, F. Marchesoni, E. Marinari, G. Parisi, L. Peliti, S. Ruffo, and A. Vulpiani, Approach to equilibrium in a chain of nonlinear oscillators, J. Phys. (France) **43**, 707 (1982).

[31] See Supplemental Material at http://link.aps.org/supplemental/10.1103/PhysRevE.95.060202 for the comparison between the computed equipartition times and those showed in Ref. [26] and the fitting procedure used to exponent the exponent of the tails of the PDFs.

[32] Numerical simulations presented in this Rapid Communication have been performed on the Massey Cluster Simurg, which uses Intel Xeon CPU E5-2670 processors, and on the PCS-IBS Cluster, which uses Intel E5-2680v3 processors.

[33] B. V. Chirikov and D. L. Shepelyansky, in *Proceedings of the IXth International Conference on Nonlinear Oscillations*, Kiev, 1981 (Naukova Dumka, Kiev, 1984), Vol. 2, pp. 421–424 (English translation: Statistics of Poincaré recurrences and the structure of the stochastic layer of a nonlinear resonance, Princeton University Report No. PPPL-TRANS-133, 1983).

[34] C. F. F. Karney, Long-time correlations in the stochastic regime, Physica D **8**, 360 (1983).

[35] M. Ding, T. Bountis, and E. Ott, Algebraic escape in higher dimensional Hamiltonian systems, Phys. Lett. A **151**, 395 (1990); E. G. Altmann and H. Kantz, Hypothesis of strong chaos and anomalous diffusion in coupled symplectic maps, Europhys. Lett. **78**, 10008 (2007); S. Lange, A. Bäcker, and R. Ketzmerick, What is the mechanism of power-law distributed Poincaré recurrences in higher-dimensional systems? *ibid.* **116**, 30002 (2016).